RSC Advances

PAPER

View Article Online
View Journal | View Issue

Cite this: *RSC Adv.*, 2019, **9**, 26224

Structure confirmation and thermal kinetics of the inclusion of *cis*-jasmone in β-cyclodextrin

Lvye Ai,[a] Jingyan Hu,[a] Xiaoming Ji *[a] and Huaxin Zhao*[b]

Received 5th May 2019
Accepted 1st August 2019

DOI: 10.1039/c9ra03343b

rsc.li/rsc-advances

In this study, inclusion complex of *cis*-jasmone in β-CD (β-CD-CJ) was synthesized to improve *cis*-jasmone stability. The structure and thermal kinetics of the inclusion complex was investigated by Fourier transform infrared spectroscopy (FTIR), thermogravimetric analysis (TG) and differential scanning calorimetry (DSC). DSC studies showed that the stability of *cis*-jasmone after β-cyclodextrin encapsulation was improved. The dissociation kinetics of β-CD-CJ at different heating rates was studied by TG, and the activation energy *E* of β-CD-CJ thermal decomposition kinetic parameters was defined by Flynn–Wall–Ozawa method. The results showed that the average activation energy *E* was 121.16 kJ mol^{-1}.

1. Introduction

β-Cyclodextrin (β-CD) is a cone-shaped cavity polymer consisting of seven glucopyranose units linked by α-(1,4) bonds.[1] The cone-shaped cavity of β-CD allows the accommodation of the different classes of molecules to form inclusion complexes for the purpose of increasing solubility and stability.[2–7] The inclusion complexes are constituted by a host molecule and a variety of guest molecules. In addition to slight deformation, the size and shape of the available cavity of the host molecules and the structural features of the guest molecules are almost unchanged.[8] The capability of cyclodextrins for complex formation depends on the guest molecule's size, which should fit inside the cavity of cyclodextrin, and on thermodynamic interactions between cyclodextrins guest molecule, and the solvent.[9] Therefore β-CD is typically used as a host molecule encapsulating agent for food additives, flavorings, vitamins and pharmaceutical development.[8,10] After being encapsulated by β-CD, the physical, chemical and biological properties of molecules may be modified. For instance, β-CD acts as a flavor sealant to protect against oxidation, or reduce unwanted taste.[11] Inclusion complex of *trans*-cinnamaldehyde in β-CD is blended with chitosan to treat fresh-cut melon, which can effectively maintain the hardness and color of melon, reduce weight loss and prolong shelf life.[12] Inclusion complexes between drug and (β-CD) can increase the apparent aqueous solubility and enhance bioavailability of the drug.[13] Carvalho *et al.* used two different techniques to prepare inclusion complexes between FZD and β-cyclodextrin (β-CD), and physicochemical analysis revealed the inclusion complexes could be used in the pharmacotherapy of leishmaniasis in dogs infected with *L. amazonensis*.[14] What's more, β-CD is a safe natural inclusion material.[15,16] The inclusion complex of cyclodextrin and perfume molecules can improve the water solubility of perfume molecules, increase the stability of perfume molecules, and improve the availability of perfume molecules. Extend the fragrance period and improve the quality of the product.[17] *Cis*-jasmone is widely available in jasmine, orange blossom, bergamot, sea tong, kiwi, honeysuckle, magnolia, lotus root, and tobacco.[18–21] It is repellent to aphids and reduces secondary metabolites of pest's development.[22–24] Moreover, *cis*-jasmone is the most important contribution to the scents of perfumes and cosmetics.[25] Therefore, *cis*-jasmone has received more and more attention. However, the scent of the *cis*-jasmone is extremely volatile and their fragrance is easily lost. The instability limits the application of *cis*-jasmone. The complexity of *cis*-jasmone in β-CD (β-CD-CJ) was rarely reported in the literature before, let alone the thermal dissociation kinetics of them. The aim of this study was to prepare and characterize β-CD-CJ, providing a way to increase the stability of the *cis*-jasmone. In this work, β-CD-CJ was prepared under controlled experimental conditions.[26] Then the inclusion complex was characterized by FTIR. Finally, the thermal dissociation kinetics of the inclusion complex was evaluated.

2. Materials and methods

2.1. Materials

Cis-jasmone, 97%, was purchased from Henan Xinzheng Gold Leaf Spice Co., Ltd (China) and was without further purification. β-Cyclodextrin was purchased from Tianjin Kermel Chemical Reagent Co., Ltd (China).

2.2. Preparation of β-CD-CJ

β-CD-CJ was prepared by adding the *cis*-jasmone to a saturated β-CD solution in a molar ratio (β-CD: *cis*-jasmone) of 1 : 2, at 60 °C for 6 h, then slowly reduced the temperature of the reaction to 4 °C. After 24 h, the reaction solution was filtered, then the solid was washed with distilled water and ethanol,

[a]*College of Tobacco Science, Henan Agricultural University/Henan Province Flavors & Perfumes Engineering Research Center, Zhengzhou 450002, China. E-mail: jxm0371@163.com; xiaomingji@henau.edu.cn; Tel: +86-371-63555713*

[b]*College of Life Science, Henan Agricultural University, Zhengzhou 450002, China. E-mail: zhaohuaxin2010@126.com; Tel: +86-371-63558682*

respectively. Afterward the solid was dried under vacuum and stored in an airtight glass vessel. This method resembles that previously described in literature.[27]

2.3. Methods

The samples (β-CD, *cis*-jasmone, β-CD-CJ, a mixture of β-CD and *cis*-jasmone (molar ratio 1 : 1)) were analyzed by FTIR (Nicolet iS50), samples and spectroscopic-grade KBr were compressed into a 1 mm wafer. For each sample scanning range was from 4000 to 400 cm^{-1} and a resolution of 4 cm^{-1}.

Thermal analysis was carried out using a simultaneous thermal analyzer (NETZSCH STA 449 F3, Germany). Spectroscopic pure Al_2O_3 was taken as a reference substance, and Ar_2 was used as protective gas (flow rate 60 mL min^{-1}) and purge gas (flow rate 20 mL min^{-1}). Thermal degradation temperature ranged from 30 to 900 °C. The mass of each sample used for DSC and TG analysis was approximately 10 mg. The heating rate of the precursor materials (β-CD, *cis*-jasmone), a mixture of β-CD and *cis*-jasmone (MCJ) and β-CD-CJ were 10 K min^{-1}. Furthermore, two heating rates, 5 K min^{-1} (Φ_1) and 20 K min^{-1} (Φ_3), have been used to measure thermogravimetric of β-CD-CJ.

3. Results and discussion

3.1. Structure identification

The infrared characterization curves of the samples are illustrated in Fig. 1 curves (a), (b), (c) and (d) are infrared characteristic peaks of β-CD, *cis*-jasmone, MCJ and β-CD-CJ, respectively. Among the Fig. 1, it is clear that the infrared characteristic peaks of *cis*-jasmone and β-CD can be found in the curve (c), indicating that MCJ is just a simple mixture of β-CD and *cis*-jasmone. Compared with the curve (c), the number of peaks shown in the curve (d) is reduced, the peak strength is weakened, and the shape of the peak becomes wider. Moreover, the characteristic peak of *cis*-jasmone carbonyl group had an obviously decrease in the intensity of the peak at 1698 cm^{-1} and 1645 cm^{-1}, 1698 cm^{-1} for C=O stretching vibration this data is similar to that previously described in literature,[28] 1645 cm^{-1} for C=C stretching vibration, indicating that these part of the carbonyl group and carbon–carbon double bond are likely to be inserted into the cone-shaped cavity of β-CD.

3.2. Thermal analysis

3.2.1. TG analysis. The TG and DTG curves of samples for the heating rate of 10 K min^{-1} are indicated from Fig. 2–5. The curves profile of Fig. 2 suggests that the process of thermal decomposition of *cis*-jasmone occurred apparently in two steps. From 30 to 200 °C, *cis*-jasmone exhibited a sharp decrease with a mass loss of 97.33%. The second stage exhibited a slow mass loss process with mass loss of 2.15%. Within the temperature of 30–200 °C, the DTG profile of *cis*-jasmone exhibited two peaks temperature ($T_{p,1}$ = 135 °C, $T_{p,2}$ = 175.5 °C).

The relationship between temperature change and mass loss of β-CD is illustrated in Fig. 3. It revealed that three stages of the thermal degradation of β-CD can be observed, with temperature increasing. The first stage occurred in the temperature range of 30 to 300 °C, and the mass loss of β-CD was about 23.09%. At this stage, there was one peak temperature on the top of the DTG curve ($T_{p,1}$ = 100 °C). The second stage mass loss started at 300 °C and ended at 375 °C. This was the main mass loss stage as indicated and total mass loss was 74.6%. The DTG profile of β-CD depicted one obvious peak temperature ($T_{p,2}$ = 322.5 °C). From 375 °C to 900 °C, the TG curve became flat, which showed the residual carbonaceous material of the former steps.

The MCJ had undergone four major mass loss stages was presented in Fig. 4. From 30 to 345 °C, MCJ had three consecutive mass loss processes, with a total mass loss of 74.6%. During this process, the DTG curve of MCJ shows two evident peak temperatures ($T_{p,1}$ = 195 °C, $T_{p,2}$ = 325 °C).

The TG and DTG curves of the β-CD-CJ were shown in Fig. 5. As can be seen from the TG curve, there were three stages of thermal decomposition, the first step of decomposition occurred from 30 to 227.5 °C, there was almost no loss of mass, meaning that β-CD-CJ was almost not decomposed. The second mass loss step began at 227.5 and ended at 360 °C, the TG

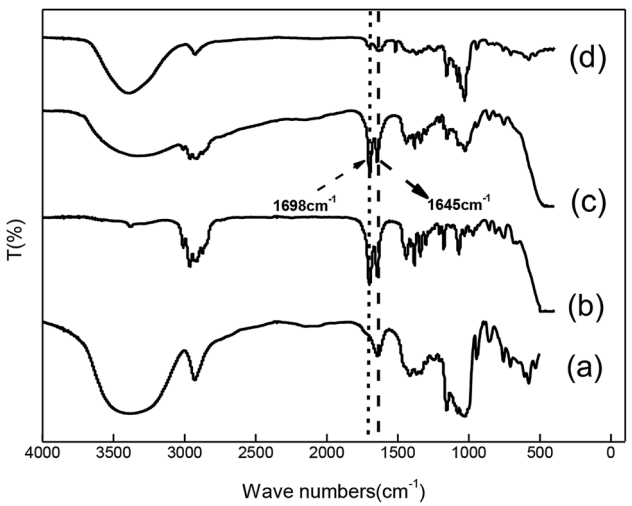

Fig. 1 FTIR for: (a) β-CD; (b) *cis*-jasmone; (c) MCJ; (d) β-CD-CJ.

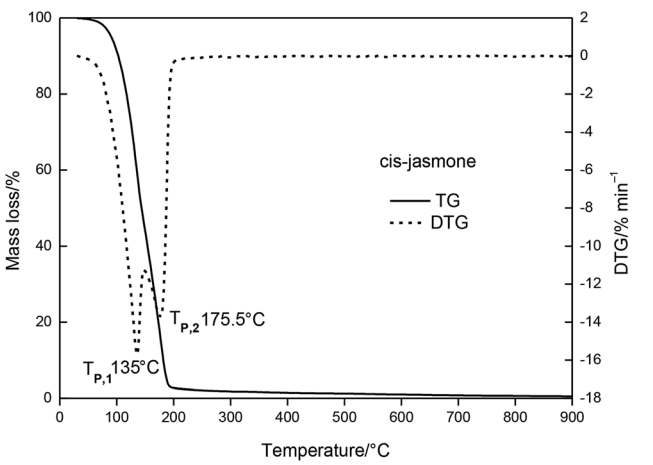

Fig. 2 TG and DTG curves of *cis*-jasmone.

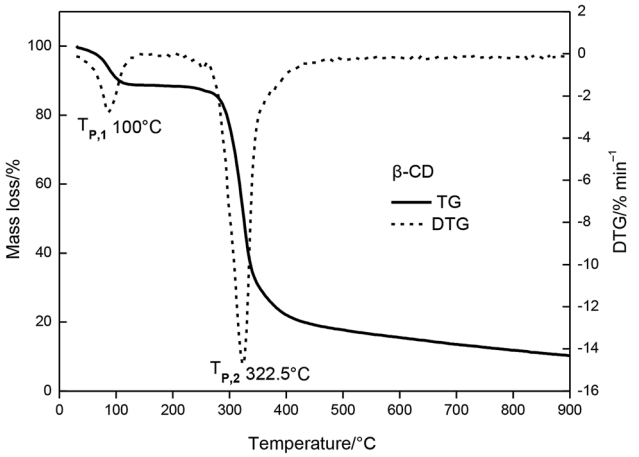

Fig. 3 TG and DTG curves of β-CD.

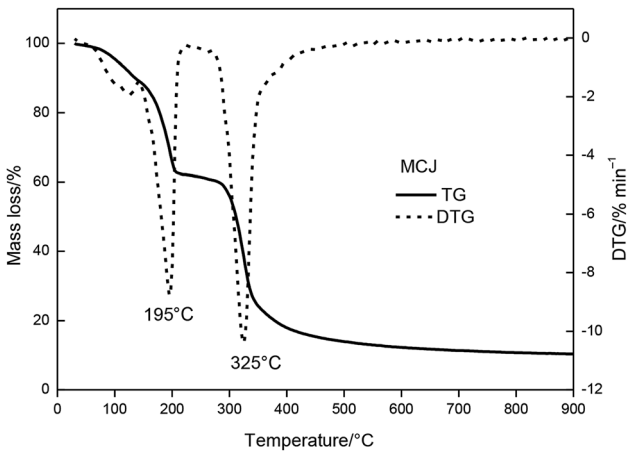

Fig. 4 TG and DTG curves of MCJ.

curves depict a very sharp decrease loss process with mass loss of 76.3% of original mass. In this stage, the DTG curve of β-CD-CJ had only one peak temperature ($T_{p,1}$ = 327 °C). After 360 °C, TG curve became stable and the mass loss was about 4.1% of the original mass.

The results indicated that the thermal stability of *cis*-jasmone was improved after encapsulation, because the decomposition reaction of β-CD-CJ began at 227.5 °C, in contrast to *cis*-jasmone which thermal decomposition started at 30 °C. It was observed that the mass loss of decomposition of β-CD-CJ (76.3%) was lower than that of *cis*-jasmone (97.33%), indicating the inclusion effect was effective.

3.2.2. DSC analysis. The results shown in the TG, DTG and DSC curves coincide with each other. The onset temperatures and peak temperatures of the samples were recorded by DSC curves. Fig. 6 and 7 show that the onset temperatures of thermal decomposition of *cis*-jasmone and β-CD were 137.5 °C, 90.8 °C, and the T_{peak} of *cis*-jasmone and β-CD measured by DSC was 185 and 297.7 °C, respectively. The DSC results for MCJ and β-CD-CJ are shown in Fig. 8 and 9, respectively. DSC measured the thermal decomposition onset temperature of MCJ was 103.5 °C, and the T_{peaks} were 198.6 and 280.2 °C, respectively. However, β-CD-CJ has only one T_{peak} temperature of 307.1 °C. This further demonstrated that β-CD-CJ was not a mixture of *cis*-jasmone and β-CD, but an inclusion complex of *cis*-jasmone in β-CD.

3.3. Kinetic analyses

The TG curves of thermal decomposition of β-CD-CJ with various heating rates were shown in Fig. 10. That can be seen from the figure, with the heating rate increasing, the TG curve moves to the right. The reason for it because the different heating rates affects mass loss rates of the β-CD-CJ, as well as high heating rates effectively facilitates the thermal decomposition reaction of the inclusion complex.

The simple thermal decomposition reaction equation[24] is as follows:

$$\ln \ln(1/(1 - a)) = -E/RT + b \quad (1)$$

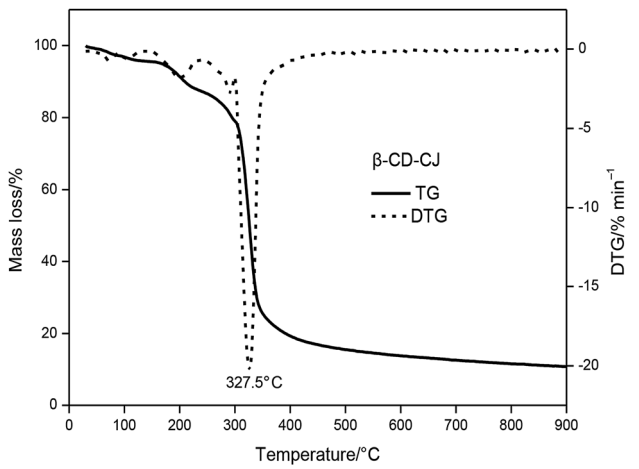

Fig. 5 TG and DTG curves of β-CD-CJ.

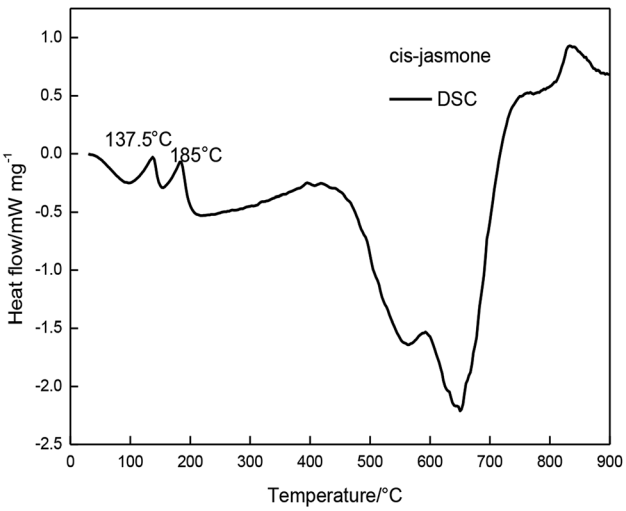

Fig. 6 DSC curve of *cis*-jasmone.

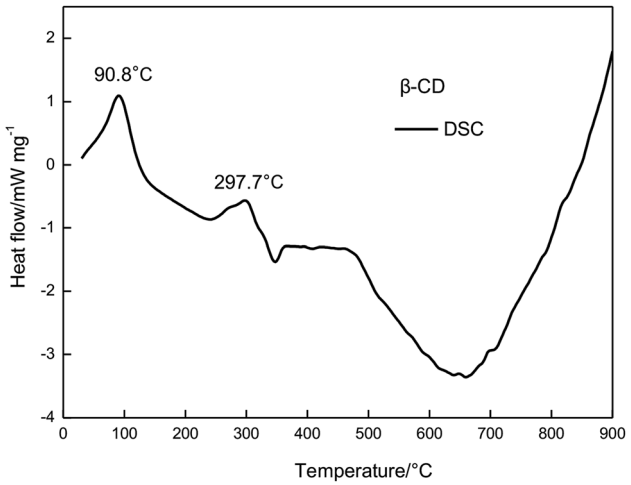

Fig. 7 DSC curve of β-CD.

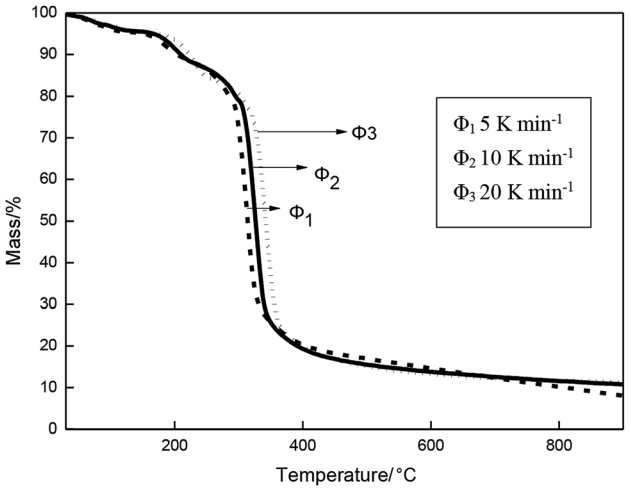

Fig. 10 TG curves of β-CD-CJ in different heating rate.

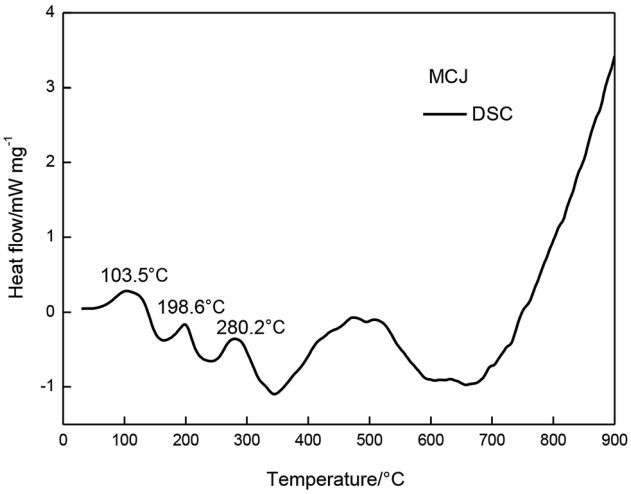

Fig. 8 DSC curve of MCJ.

When the reaction order is 1, the plot of $\ln \ln(1/(1-a))$ against $1/T$ is a straight line. When the reaction order is less than 1, the lower half of the straight line is shifted to the left, otherwise, it moves to the right.

The kinetics of any solid-state decomposition reaction can be defined by the Flynn–Wall–Ozawa method[29,30] as shown in the following:

$$\log \Phi = \log(-AE/Rf(a)) - 2.315 - 0.4567(E/RT) \quad (2)$$

When $n = 1$, eqn (2) can be converted into the following form:

$$\log \Phi = \log(-AE/R\ \ln(1-a)) - 2.315 - 0.4567(E/RT) \quad (3)$$

where b is a constant, T is temperature (K), a is mass loss rate, E is activation energy (J mol^{-1}), R is gas constant (8134 J mol^{-1} K^{-1}) and Φ is the heating rate (K min^{-1}), $f(a) = \int da/(1-a)^n$, (n

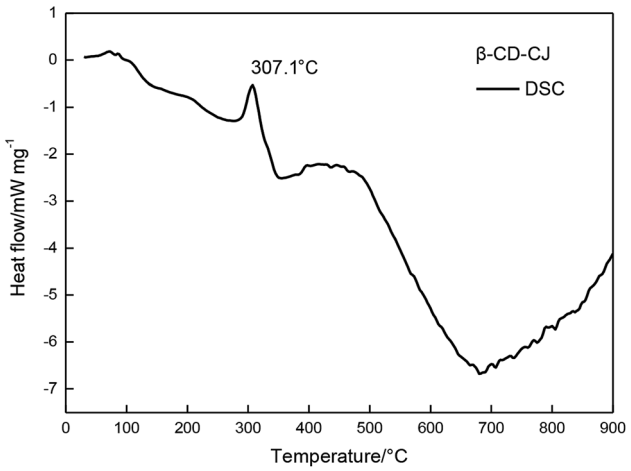

Fig. 9 DSC curve of β-CD-CJ.

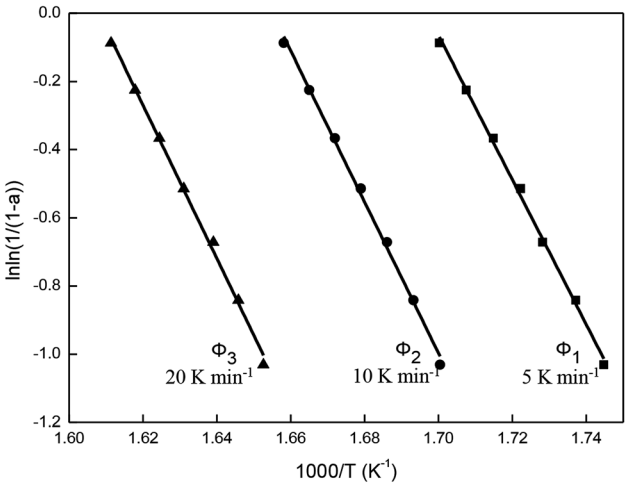

Fig. 11 The relation of [ln ln(1/(1 − a))] and [1/T] in different heating rate.

Table 1 Temperatures corresponding to the same mass loss in different heating rate

	T (K)		
a	5 (K min^{-1})	10 (K min^{-1})	20 (K min^{-1})
0.30	573.15	588.1	605.1
0.35	575.65	590.6	607.6
0.40	578.65	593.1	610.1
0.45	580.65	595.6	613.1
0.50	583.15	598.1	615.6
0.55	585.65	600.6	618.1
0.60	588.15	603.1	620.6

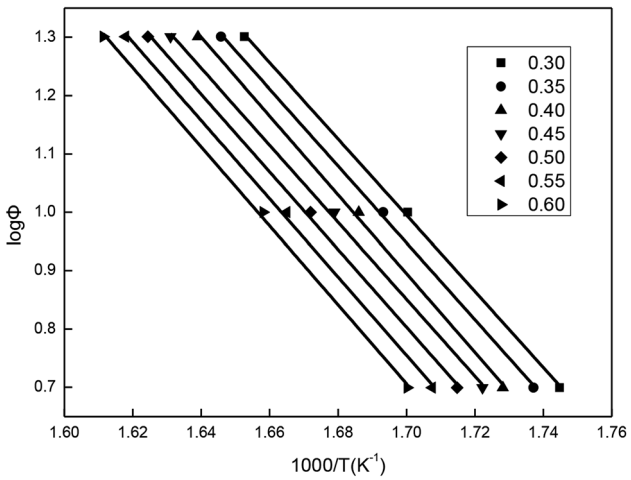

Fig. 12 Plots of the kinetics analysis based on the Ozawa method.

is the number of reaction order). If the plot of ln Φ against $1/T$ is linear, the activation energy E and pre-exponential factor A can be calculated from the slope and intercept, respectively.

Fig. 11 is obtained according to eqn (1). As shown, ln ln$(1/(1-a))$ and $1/T$ exhibited straight lines relationship, indicating the thermal decomposition of β-CD-CJ is a first-order reaction.

The values of temperatures (T) at the same mass loss (a) on three TG curves of the β-CD-CJ are summarized in Table 1. By substituting the values of Φ and T in Table 1 into eqn (3), the slope and the intercept at the different mass loss rate were achieved by the linear least squares method with [log Φ] *versus* [$1/T$]. The results received were presented in the Fig. 12 and the Table 2. Judging from the results of Table 2, the average activation energy of β-CD-CJ was 121.16 kJ mol^{-1}. The lower activation energy value indicated that there was no strong chemical bond between β-CD and the guest molecule *cis*-jasmone. The host molecule and the guest molecule were mainly based on van der Waals force.[31,32]

Table 2 The values of the kinetic parameters computed by the Flynn–Wall–Ozawa method

Sample	a	Slope	Intercept	E (kJ mol^{-1})	A
β-CD-CJ	0.30	−6.53228	12.09999	118.89	6.48×10^{12}
	0.35	−6.58786	12.14706	119.90	8.65×10^{12}
	0.40	−6.75153	12.37249	122.88	1.68×10^{13}
	0.45	−6.59913	12.06948	120.10	1.00×10^{13}
	0.50	−6.65454	12.11579	121.11	1.28×10^{13}
	0.55	−6.71019	12.1621	122.13	1.63×10^{13}
	0.60	−6.76606	12.20841	123.14	2.06×10^{13}
Average activation energy E (kJ mol^{-1})				121.16	

4. Conclusion

In FTIR analysis, the structure of the inclusion complex was monitored by the changes of the carbonyl indexes which indicated the structural characteristics of *cis*-jasmone after encapsulation. The results showed that the carbonyl peak intensity of the inclusion complex was significantly lower than the carbonyl peak intensity of *cis*-jasmone.

TG and DTG curves showed that the mass loss of the β-CD-CJ was less than *cis*-jasmone. DSC curves demonstrated that the β-CD-CJ has only one T_{peak} temperature of 307.1 °C.

The results of the kinetic analysis indicated that the thermal decomposition of β-CD-CJ was dominated by a first-order thermal decomposition reaction process. The average activation energy for the process was 121.16 kJ mol^{-1}. The average activation energy in the range of 40 kJ mol^{-1} to 400 kJ mol^{-1} belongs to chemical reaction control process.[33]

In a nutshell, *cis*-jasmone could form a stable inclusion complex with β-CD was revealed by FTIR, TG/DTG and DSC, and the thermal stability of *cis*-jasmone was improved by encapsulation, which provided some theoretical basis for the application of *cis*-jasmone.

Conflicts of interest

There are no conflicts to declare.

Acknowledgements

This work was supported by Ministry of Agriculture and Rural Affairs of the People's Republic of China (No. 2017YFD0200808); Hubei China Tobacco Industry Limited Liability Company (2018420000340440); Fujian Tobacco Company Longyan City Company (201835080027071).

References

1 P. Dąbrowska and W. Boland, *ChemBioChem*, 2007, **8**, 2281–2285.
2 R. A. Rajewski and V. J. Stella, *J. Pharm. Sci.*, 1996, **85**, 1142–1169.
3 L. M. Pinto, L. F. Fraceto, M. H. Santana, T. A. Pertinhez, S. O. Junior and E. de Paula, *J. Pharm. Biomed. Anal.*, 2005, **39**, 956–963.
4 D. Duchêne, C. Vaution and F. Glomot, *Drug Dev. Ind. Pharm.*, 1986, **12**, 2193–2215.
5 G. Dollo, D. O. Thompson, P. L. Corre, F. Chevanne and R. L. Verge, *Int. J. Pharm.*, 1998, **164**, 11–19.

6 S. L. Xin, W. H. Ming, Z. Z. Qiang and Q. Q. Liu, *Bull. Chem. Soc. Jpn.*, 2007, **80**, 2313–2322.
7 W. Eli, W. Chen and Q. Xue, *J. Inclusion Phenom. Macrocyclic Chem.*, 2000, **36**, 439–445.
8 F. K. Heinz and J. Szejtli, *Cyclodextrin Inclusion Complexes*, 1988, pp. 79–185.
9 E. M. M. D. Vall, *Process Biochem.*, 2004, **9**, 1033–1046.
10 V. M. Rao and V. J. Stella, *J. Pharm. Sci.*, 2003, **92**, 927–932.
11 J. S. Yu, F. D. Wei, W. Gao and C. C. Zhao, *Spectrochim. Acta, Part A*, 2002, **58**, 249–256.
12 J. N. Patel, D. M. Rathod, N. A. Patel and M. K. Modasiya, *Int. J. Pharm. Life Sci.*, 2012, **2**, 1459–1469.
13 S. P. Moreira, W. M. Carvalho and A. C. Alexandrino, *Int. J. Food Sci. Technol.*, 2015, **10**, 2192–2203.
14 S. G. Carvalho, L. A. Siqueira, M. S. Zanini and A. P. dos Santos Matos, *Res. Vet. Sci.*, 2018, **119**, 143–153.
15 S. Z. Zhang and X. H. Wang, *Microbiology*, 1988, **4**, 65–66.
16 J. W. Lei, X. F. Wu and X. G. Cui, *China J. Chin. Med.*, 2011, **1**, 59–61.
17 B. Yang and G. Yang, *Sci. Technol. Food Ind.*, 2007, **1**, 210–212.
18 L. Ruzicka and M. Pfeiffer, *Helv. Chim. Acta*, 1933, **16**, 1208–1214.
19 T. Koch, K. Bandemer and W. Boland, *Helv. Chim. Acta*, 1997, **80**, 838–850.
20 J. B. Harborne, *Phytochemistry*, 1995, **39**, 954.
21 J. T. Knudsen, L. Tollsten and L. G. Bergström, *Phytochemistry*, 1993, **33**, 253–280.
22 M. A. Birkett, C. A. M. Campbell and K. Chamberlain, *Proc. Natl. Acad. Sci. U. S. A.*, 2000, **97**, 9329–9334.
23 T. J. A. Bruce, J. L. Martin, J. A. Pickett, B. J. Pye, L. E. Smart and L. J. Wadhams, *Pest Manage. Sci.*, 2010, **59**, 1031–1036.
24 J. A. Pickett, M. A. Birkett and T. J. A. Bruce, *Pestic. Outlook*, 2005, **14**, 96–98.
25 V. T. Karathanos, I. Mourtzinos, K. Yannakopoulou and N. K. Andrikopoulos, *Food Chem.*, 2007, **101**, 652–658.
26 M. M. Meier, M. T. B. Luiz, B. Szpoganicz and V. Soldi, *Thermochim. Acta*, 2001, **1**, 153–160.
27 G. P. Luo, M. R. Yan, H. N. Meng and C. Chen, *China Food Addit.*, 2019, **30**, 70–76.
28 J. Men, L. Wang, Y. H. Li, T. Li, M. Tang and F. C. Gu, *Chem. Ind. Eng.*, 2006, **23**, 215–219.
29 Y. He and T. Sun, *Food Sci.*, 2006, **2**, 25–28.
30 T. Ozawa, *Bull. Chem. Soc. Jpn.*, 1965, **38**, 1881–1886.
31 S. J. Tian, G. X. Xi, Q. T. Cheng, X. D. Lou and H. J. Li, *J. Therm. Anal. Calorim.*, 1998, **53**, 825–833.
32 M. R. Caira, S. A Bourne and E. Mvula, *J. Therm. Anal. Calorim.*, 1999, **56**, 1329–1334.
33 G. Q. Hu, P. P. Wu, B. H. Xie and S. J. Zhang, *J. Zhengzhou Univ.*, 2014, **35**, 73–76.